

Resonance Propagation and Mitigation in Grid-Connected and Islanding Microgrids by Using fuzzy Logic

T.Prasanna

**Pursuing M.Tech, PE Branch,
Dept of EEE,**

Vinuthna Institute of Technology Science, Warangal.

Pulicheru Ravi

**Associate Professor,
Dept of EEE,**

Vinuthna Institute of Technology Science, Warangal.

Abstract:

In this paper, a microgrid resonance propagation model is investigated. To actively mitigate the resonance using DG units, an enhanced DG unit control scheme that uses the concept of virtual impedance is proposed. It can be seen that a conventional voltage-controlled dg unit with an LC filter has a short-circuit feature at the chosen harmonic frequencies, whereas a current-controlled dg unit presents an open-circuit characteristic. because of completely different behaviors at harmonic frequencies, specific harmonic mitigation methods shall be developed for current controlled and voltage-controlled dg units, respectively. The application of underground cables and shunt capacitor banks may introduce power distribution system resonances. This paper additionally focuses on developing a voltage-controlled dg unit-based active harmonic damping technique for grid-connected and islanding microgrid systems. an improved virtual impedance control method with a virtual damping resistor and a nonlinear virtual capacitor is proposed. The nonlinear virtual capacitor is used to compensate the harmonic dip on the grid-side inductor of a dg unit LCL filter. Here we are using fuzzy controller compared to other controller due to its accurate performance. The virtual resistance is principally answerable for microgrid resonance damping. The effectiveness of the proposed damping method is examined using each a single dg unit and multiple parallel dg units.

Index Terms:

Active power filter, distributed power generation, droop control, grid-connected converter, microgrid, power quality, renewable energy system, resonance propagation, virtual impedance.

INTRODUCTION:

The increasing application of nonlinear loads can led to significant harmonic pollution in a power distribution system. The harmonic distortion might excite complicated resonances, particularly in power systems with underground cables or subsea cables and. In fact, these cables with nontrivial parasite shunt capacitance will form an LC ladder network to amplify resonances. in order to mitigate system resonances, damping resistors or passive filters can be placed in the distribution networks . however, the mitigation of resonance propagation exploitation passive components is subject to some well understood problems, like power loss and additional investment. Moreover, a passive filter might even bring extra resonances if it's designed or installed without knowing detailed system configurations.

To avoid the adoption of passive damping equipment, numerous types of active damping methods are developed. Among them, the resistive active power filter (R-APF) is often considered as a promising way to understand better performance. Conventionally, the principle of R-APF is to emulate the behavior of passive damping resistors by applying a closed-loop current-controlled method (CCM) to power electronics converters. in this management category, the R-APF will be simply modeled as a virtual harmonic resistor if it's viewed at the distribution system level. in addition, many changed R-APF ideas were additionally developed in the recent literature. In, the separate tuning method was proposed to regulate damping resistances at different harmonic orders. Accordingly, the R-APF basically works as a nonlinear resistor.

In, the operation of multiple R-APFs was also considered, where an interesting droop control was designed to offer autonomous harmonic power sharing ability among parallel R-APFs. On the other hand, renewable energy source (RES) based distributed generation (DG) units are adopted to form flexible microgrids and their interfacing converters even have the chance to address different distribution system power quality problems. For current-controlled dg units, the auxiliary R-APF function can be seamlessly incorporated into the primary dg real power injection function by modifying the current reference. However, conventional CCM will hardly provide direct voltage support throughout microgrid islanding operation. to beat this limitation, an enhanced voltage-controlled method (VCM) was recently proposed for dg units with high-order LC or LCL filters. It can be seen that the control method in regulates the dg unit as virtual impedance, that is dependent on the present feeder electric resistance. once the feeder electric resistance is inductive, this method could not provide enough damping effects to system resonance. harmonic current at position x. The length of the feeder is l It is easy to obtain the harmonic voltage–current standing wave equations at the harmonic order k as assumed to be stiff and $V_{pcck} \cdot V_k(x)$ and $I_k(x)$ square measure the feeder kth harmonic.

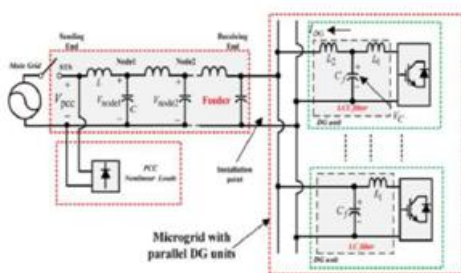


Fig. 1. Simplified one-line diagram of a single-phase microgrid. service. Simulated results are provided to confirm the validity of the proposed method.

II. MODELING OF DG UNITS IN MICROGRID SYSTEM

Fig. 1 illustrates the configuration of a single-phase microgrid system, where a few dg units are

interconnected to the point of common coupling (PCC) through an extended underground feeder. For the sake of simplicity, this paper only adopts an easy microgrid configuration to demonstrate how the microgrid power quality is affected by resonance propagation. in addition, this paper also assumes that shunt capacitor banks and parasitic feeder capacitances are equally distributed in the feeder. Note that the static transfer switch (STS) controls the operation mode of the microgrid. when the most grid is disconnected from the microgrid, the PCC nonlinear loads shall be supplied by the standalone dg units.

A. Distributed Parameter Model in Grid-Tied Operation

For a protracted feeder, as illustrated in Fig. 1, a lumped parameter model isn't able to describe its

$$V_k(x) = Ae^{-\gamma x} + Be^{\gamma x} \quad (1)$$

$$I_k(x) = \frac{1}{z}(Ae^{-\gamma x} - Be^{\gamma x}) \quad (2)$$

Resonance propagation characteristics. alternatively, the distributed parameter model was mentioned in [3] and [6], where the voltage distortions at PCC induce a harmonic voltage standing wave on the

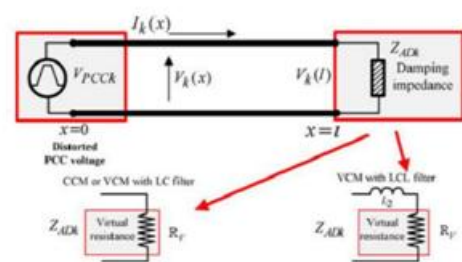


Fig. 2. Equivalent circuit of a single grid-connected DG unit at the kth harmonic frequency.

where A and B are constants, which are determined by feeder boundary conditions. z and γ are the characteristics impedance [3] of the feeder without considering the line resistance as

$$Z = \sqrt{\frac{L}{C}} \quad (3)$$

$$\gamma = jk\omega_f \sqrt{LC} \quad (4)$$

where ω_f is the fundamental angular frequency and L and C are the feeder equivalent inductance and shunt capacitance per kilometer, respectively.

1) DG Units with CCM and R-APF Control: To determine the boundary conditions of the feeder, the equivalent harmonic impedance (Z_{ADk}) of the DG unit must be derived. First, the current reference (I_{ref}) of a CCM-based DG unit can be obtained as

$$I_{ref} = i_{reff} - I_{AD} = I_{reff} - \frac{H_D(s)V(l)}{R_V} \quad (5)$$

where I_{reff} is the fundamental current reference for DG unit power control, I_{AD} is the harmonic current reference for system resonance compensation, $V(l)$ is the measured installation point voltage at the receiving end of the feeder, $H_D(s)$ is the transfer function of a harmonic detector, which extracts the harmonic components of the installation point voltage, and R_V is the command virtual resistance.

$$\begin{aligned} \omega_{DG} &= \omega_f + D_p \cdot (P_{ref} - P_{LPF}) \\ E_{DG} &= E + D_q \cdot (Q_{ref} - Q_{LPF}) + \frac{K_Q}{S} (Q_{ref} - Q_{LPF}) \end{aligned} \quad (6)$$

where ω_f and ω_{DG} are the nominal and reference angular frequencies. E and E_{DG} are the nominal and reference DG voltage magnitudes. P_{LPF} and Q_{LPF} are the measured power with lowpass filtering. D_p and D_q are the droop slopes of the controller. Note that with the integral control to regulate DG unit voltage magnitude in (7), the steady-state reactive power control error at the grid-tied operation is zero. Once the voltage magnitude reference and the frequency reference are determined, the ripple-free instantaneous voltage reference (V_{reff}) can be easily obtained. The equivalent impedance of VCM-based DG unit with an LC filter has already been tuned to be resistive, by adding a DG line current (I_{DG}) feed-forward term to the voltage control reference. Although previous VCM-based DG equivalent impedance shaping techniques mainly focus on improving the power sharing performance of multiple DG units in an islanding microgrid, similar idea can also be used to mitigate the harmonic propagation along the feeder as

$$\begin{aligned} V_{ref} &= V_{reff} - V_{AD} \\ &= V_{reff} - R_V \cdot (H_D(s) \cdot I_{DG}) \end{aligned} \quad (8)$$

where V_{reff} is the fundamental voltage reference derived from droop control in (6) and (7), V_{AD} is the harmonic voltage reference for DG unit harmonic impedance shaping, I_{DG} is the measured DG unit line current (see Fig. 1), $H_D(s)$ is the transfer function of a harmonic detector, which extracts the harmonic components of DG unit line current, and R_V is the virtual resistance command. Note that when a VCM-based DG unit with an LC filter is controlled without any harmonic impedance shaping target [by setting $R_V = 0$ in (8)], it essentially works as short-circuit connection ($Z_{ADk} = 0$) at the harmonic frequencies. Nevertheless, if an LCL filter is adopted as the DG output filter, the VCM-based control method using filter capacitor voltage regulation does not address the harmonic voltage drop on the grid-side inductor (L_2). Accordingly, the DG unit shall be modeled as the combination of a reactor and a resistor ($Z_{ADk} = R_V + jk\omega_f L_2$) when (8) is applied to the DG unit (see Fig. 2). As will be discussed later, the imaginary part of Z_{ADk} may affect the voltage harmonic suppression performance of the system. Since a grid-connected DG unit using either CCM or VCM can be modeled by an equivalent harmonic impedance at the receiving end of the feeder, the following boundary conditions can be obtained

$$\frac{V_k(l)}{I_k(l)} = Z_{ADK} \quad (9)$$

$$V_k(0) = V_{PCCK} \quad (10)$$

By solving (1), (2), (9), and (10), the harmonic voltage propagation at the harmonic order k can be expressed as

$$V(x)_k = \frac{Z_{ADK} \cos h(\gamma(l-x)) + z \sin h(\gamma(l-x))}{Z_{ADK} \cos h(\gamma l) + z \sin h(\gamma l)} V_{PCCK} \quad (11)$$

With the obtained equation in (11), the impact of DG active damping scheme to the harmonic voltage propagation along the feeder can be easily analyzed. Note that when the microgrid feeder is purely RL impedance, the DG unit can still work as a virtual harmonic resistor at the end of the feeder.

In this case, the DG unit has the capability of absorbing some PCC nonlinear load current if it is designed and controlled properly.

B. Distributed Parameter Model in Islanding Operation

The previous section focuses on the analysis of grid-tied DG units. For an islanding microgrid system, the VCM operation of DG units is needed for direct voltage support. To the best of the authors' knowledge, the quantitative analysis of islanding microgrid harmonic propagation is not available. When only a single DG unit is placed in the islanding system, constant voltage magnitude and constant frequency (CVMCF) control can be used.

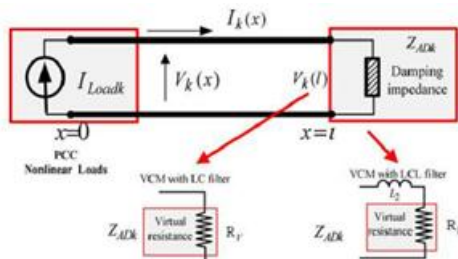


Fig. 3. Equivalent circuit of a single islanding DG unit at the kth harmonic frequency.

On the other hand, for the operation of multiple DG units in the microgrid (see Fig. 1), the droop control method in (6) and (7) [by setting $KQ = 0$ in (7)] shall be employed to realize proper power sharing among these DG units. Considering the focus of this section is to investigate the harmonic voltage damping in a stand-alone islanding system, a single DG unit at the receiving end of the feeder is considered. The circuit model of an islanding system at the harmonic order k is illustrated in Fig. 3. With the knowledge of boundary conditions at both sending and receiving ends as

$$I_k(0) = I_{Loadk} \quad (12)$$

$$\frac{V_k(l)}{I_k(l)} = Z_{ADK} \quad (13)$$

The k th harmonic voltage distortion along the feeder can be obtained

$$V_k(x) = \left(\frac{e^{-\gamma x}}{1 + ((z - Z_{ADK}) / (z + Z_{ADK})) e^{2\gamma l}} - \frac{e^{\gamma x}}{1 + ((z + Z_{ADK}) / (z - Z_{ADK})) e^{2\gamma l}} \right) Z_{Load} \quad (14)$$

From (14), it can be noticed that the voltage propagation in an islanding system harmonic is also related to the DG-unit equivalent harmonic impedance. In order to maintain satisfied voltage quality, the equivalent harmonic impedance of islanding DG units shall also be properly designed.

III. EVALUATION OF DAMPING PERFORMANCE

In this section, the performance of VCM-based DG units at different operation modes is investigated.

A. Evaluation of a Single DG Unit at the End of the Feeder

1) Grid-Tied Operation: first, the performance of a grid-tied dg unit with an LCL filter is investigated. The system parameters are unit listed in Table I. Fig. 4 shows harmonic voltage distortions on a 6 kilometer feeder. The harmonic voltage distortion issue here is normalized to the voltage distortions at PCC as $V(x)_k / V_{PCCk}$. when the conventional VCM while not damping

TABLE I: FEEDER PARAMETERS

System Parameter	Value
Feeder length	6 km
Number of nodes	7
Line inductance L	1 mH/km
Capacitance C	20 μ F/km
DG unit parameter	Value
With LCL filter	$L_1 = 2\text{mH}$ $L_2 = 3.5\text{mH}$ $C_f = 20\mu\text{F}$
Command virtual resistance	$RV = 5.5 \omega$

Is applied to the dg unit, the LCL filter condenser voltage is ripple free and the dg unit works as an inductor (L_2) at the harmonic frequencies. It is seen that the feeder is sensitive to seventh harmonic voltage distortion at the PCC. once the dg unit is controlled by the changed voltage control reference as shown in (8), it works as an equivalent RL impedance at the receiving end of the feeder. consequently, the most obvious seventh harmonic voltage propagation is effectively reduced as shown in Fig. 4(c).

Once a metric weight unit unit is coupled to the distribution system with an LC filter, the dg unit is like a harmonic damping resistor by the control scheme in (8). The corresponding performance of the system at different harmonic orders is additionally investigated in Fig. 4. once a virtual harmonic damping resistor is placed at the end of the feeder, the voltage distortions at different positions of the feeder is nearer to the harmonic voltage content at PCC. Note that for a CCM-based dg unit using the harmonic compensation scheme in (5), the dg unit is additionally like a harmonic resistor at the harmonic frequencies.

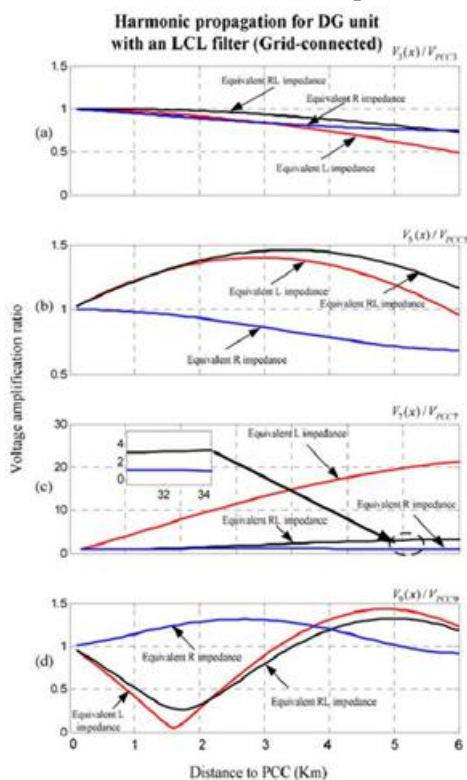


Fig. 4. Harmonic voltage amplification in a single DG unit grid-connected operation [(a)–(d): amplification ratio at 3rd, 5th, 7th, and 9th harmonic frequencies].

Therefore, the obtained waveforms can be used to evaluate the performance of CCM-based DG units in a similar way. 2) Stand-alone Operation: In addition, a DG unit with an LCL filter in a standalone islanding system is also examined. In contrast to the performance during grid-tied operation, the voltage distortion at PCC is not stiff in this case and it is

dependent on the harmonic current from the PCC nonlinear loads. As a result, the harmonic voltage amplification factor $V(x)_k/V_{PCCk}$ that is used in grid-tied systems is not very appropriate for an islanded system. Alternatively, the feeder harmonic voltage over PCC load harmonic current $(V_k(x)/V_{Loadk})$ can be used to describe the harmonic propagation characteristic of the system. The associated harmonic propagation performance is obtained in Fig. 5. As illustrated in Fig. 5(a), the 3rd harmonic current of PCC loads induces nontrivial harmonic voltage distortions at PCC when conventional VCM-controlled DG unit without using active damping is applied. On the other hand, the active damping using RL harmonic impedance [corresponding to the DG unit with an LCL filter controlled by (8)] can effectively reduce the 3rd harmonic voltage distortion. Moreover, when only a damping resistor is placed at the end of feeder, the 3rd harmonic voltage distortion is further reduced. In addition to the performance at 3rd harmonic frequency, both equivalent R and equivalent RL impedances can effectively suppress the long feeder voltage distortions at 5th, 7th, and 9th harmonic frequencies. Note that when R impedance is used, the amplitude of harmonic voltage distortions along the feeder is closer to that at PCC.

B. Evaluation of Multiple DG Units at the End of the Feeder

The performance of a microgrid with multiple dg units is increasingly discussed in the recent literature .in addition to achieve correct power sharing among multiple dg units, realizing superior harmonic damping performance in a cooperative manner is also attractive . For parallel dg units as shown in Fig. 1, they shall share the active damping current according to their respective power rating [4]. However, phase {angle|phase|point|point in time} distinction between damping resistor[corresponding to VCM-based dg unit with an LC filter controlled by (8)] and RL damping ohmic resistance [corresponding to VCM-based dg unit with an LCL filter controlled by (8)] could bring some harmonic circulating currents.

To modify the discussion, 2 VCM controlled dg units at a similar power rating are used to equally share the harmonic current associated with the active damping control. If the dg unit with an LC filter is controlled as a harmonic damping resistor R whereas the other one with an LCL filter is regulated because the RL damping ohmic resistance, the corresponding circuit diagram at the harmonic order k may be illustrated in Fig. 6. As shown, the harmonic impedances of those 2 dg units have the same resistive part. However, for the dg unit with an LCL filter, its equivalent electric resistance conjointly has an inductive part $j\omega L_2$. The current current at kth harmonic order may be observed from the phasor diagram in Fig. 7. As incontestible, the harmonic damping current of decigram unit one is in-phase with the harmonic voltage at the receiving finish of the feeder. At the same time, this of dg unit two is lagging of the harmonic voltage $V_k(l)$. With unequal current phase angles, harmonic circulating current among dg units is

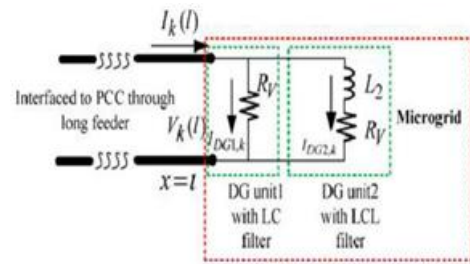


Fig. 6. Circuit diagram of a double-DG-based microgrid at the kth harmonic frequency

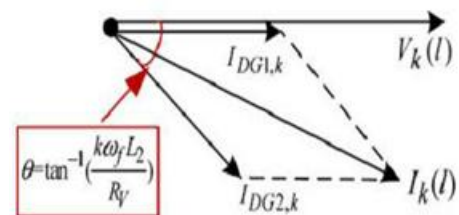


Fig. 7. Phasor diagram of the harmonic circulating current among parallel DG units.

End of the feeder is needed. In this case, microgrid equivalent harmonic impedance $Z_{ADk,microgrid}$ shall be used to replace a single DG unit equivalent harmonic impedance Z_{ADk} in (11) and (14). For a microgrid with two DG units, as shown in Fig. 6, its equivalent impedance is the parallel equivalent impedance of parallel DG units as

$$Z_{ADk,microgrid} = \frac{Z_{ADk,DG1} \cdot Z_{ADk,DG2}}{Z_{ADk,DG1} + Z_{ADk,DG2}} \quad (15)$$

IV. REALIZATION OF VIRTUAL DAMPING IMPEDANCE THROUGH DG VOLTAGE CONTROL

It has been clarified that an LCL filter grid-side inductor (L_2) can affect the performance of distribution system harmonic suppression, especially in the case of multiple DG units. In order to compensate the impact of LCL filter grid-side inductor, the harmonic voltage damping scheme as shown in (8) shall be further improved.

A. Conventional Voltage Tracking

First, a negative virtual inductor can be produced by VCM. Accordingly, the modified voltage reference is obtained as

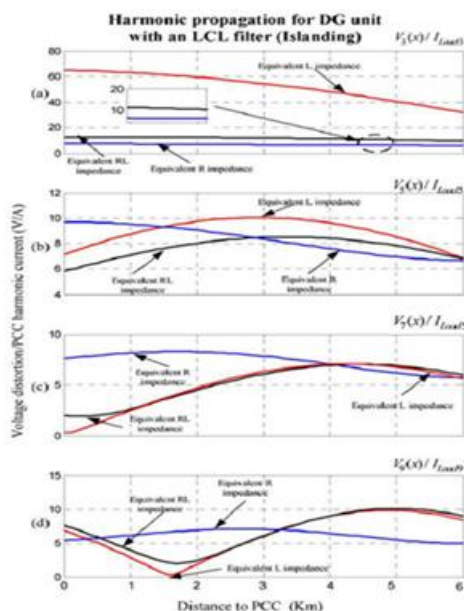


Fig. 5. Harmonic voltage amplification in a single DG unit islanding operation [(a)–(d): amplification ratio at 3rd, 5th, 7th, and 9th harmonic frequencies]. introduced. Note that to estimate the active damping current of each DG unit, the knowledge of voltage distortion $V_k(l)$ at the receiving

$$\begin{aligned}
 V_{ref} &= V_{reff} - V_{AD} - V_{comp} \\
 V_{ref} &= R_V - H_D(s) \cdot I_{DG} - s(-L_2) \cdot H_D(s) \cdot I_{DG}
 \end{aligned}
 \tag{16}$$

Comparing (16) to (8), it can be noticed that an additional voltage compensation term VComp is deducted from the voltage control reference. The aim of this voltage compensation term is to cancel the harmonic voltage drop on the grid-side LCL filter inductor L2 . Once the modified voltage reference in (16) is determined, a high bandwidth voltage controller, such as deadbeat control, H-infinity control, and multiple loop control, can be selected to ensure satisfied LCL filter capacitor voltage (VC) tracking. By further looking into (16), one can find that the implementation of virtual inductor involves derivative operation, which may adversely amplify system background noises. For instance, if a band-stop filter is selected to filter out the fundamental components as

$$H_D(S) = 1 - \frac{2\omega_{BP}S}{S^2 + 2\omega_{BP}S + \omega_f^2}
 \tag{17}$$

where ω_{BP} is the cutoff bandwidth of the band-stop filter, the voltage compensation term VComp in (16) can be expressed as

$$V_{comp} = S(-L_2) \cdot H_D(S) I_{DG} = \left(-sL_2 + \frac{2\omega_{BP}L_2S^2}{S^2 + 2\omega_{BP}S + \omega_f^2} \right) \cdot I_{DG}
 \tag{18}$$

The diagram of a DG unit with negative virtual inductor control is shown in Fig. 8. As illustrated, the DG unit is interfaced to long feeder with an LCL filter. First, the real power frequency droop control (6) and the reactive power voltage magnitude droop control (7) in the power control loop and are used to determine the fundamental voltage reference V_{reff} . Note that this droop control method can also realize proper fundamental power sharing between multiple islanding DG units, without using any communications between them. VComp in (18) is deducted from the reference voltage V_{reff} . In order to alleviate the impact of derivative operator in VComp, a highpass filter can be used as an approximation.

However, as already been pointed out in and the adoption of highpass filter introduces some magnitude and phase errors, which can degrade the performance of the compensation term VComp .

B. Implementation of Nonlinear Virtual Capacitor

In this subsection, a well-understood double-loop voltage controller is selected for DG unit voltage tracking. In the outer filter capacitor voltage control loop, the proportional and multiple resonant (PR) controllers are used as

$$\begin{aligned}
 I_{inner} &= G_{outer}(s) \cdot (V_{ref} - V_C) = \\
 &\left(K_p + \sum_K \frac{2K_{ik}\omega_c k^2}{s^2 + 2\omega_c k^2 + (k\omega_f)^2} \right) \cdot (V_{ref} - V_C)
 \end{aligned}
 \tag{19}$$

where K_P is the outer loop proportional gain, K_{ik} is the gain of resonant controller at fundamental and selected harmonic frequencies, $\omega_c k$ is the cutoff bandwidth, and I_{inner} is the control reference for the inner control loop. In the inner loop controller ($G_{inner}(s)$), a simple proportional controller (K_{inner}) is employed and the inverter output current (I_{inv}) is measured as the feedback.

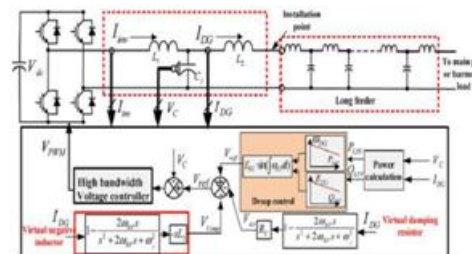


Fig. 8. Mitigation of distribution feeder harmonic propagation using virtual resistor and virtual negative inductor.

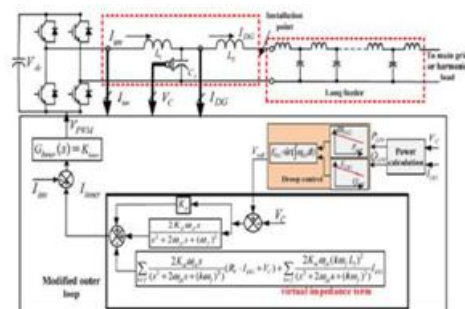


Fig. 9. Mitigation of harmonic propagation using virtual resistor and nonlinear virtual capacitor.

By further utilizing the resonant controllers in (19) to avoid the derivative operation, the paper proposes a nonlinear virtual capacitor control method instead of the use of negative virtual inductor. This is because the impedance of a capacitor also has 90° lagging phase angle, which is the same as that in a negative inductor. However, for a capacitor with fix capacitance, its impedance magnitude is in inverse proportion to harmonic orders. This feature is in contrast to the characteristics of a virtual inductor. To cancel the impacts of LCL filter grid-side inductor without using derivative operation, a nonlinear virtual capacitor with the following frequency-dependent capacitance is needed

$$L_2(\omega ft) - \frac{1}{C_{vk}(\omega ft)} = 0 \quad (20)$$

where ω is the fundamental angular frequency and C_{vt} is the command capacitance at the harmonic order t . Note that an LCL filter inductance often has some attenuation, if the line current is higher than the current rating of the filter chokes. In this case, an online estimation method can be used to identify the real-time inductance of the LCL filter and the virtual capacitance in (20) shall be modified accordingly. With the control of nonlinear virtual capacitor as shown in (20), the harmonic impact of the inductor L_2 could be properly compensated. To realize this task, the traditional harmonic detector in (17) can be replaced by a family of selective harmonic separators to extract DG line current harmonic contain (ID_{Gt}) at each selected harmonic frequency. Afterwards, the voltage drops on the nonlinear virtual capacitor can be obtained as

$$V_{comp} = \sum_t \frac{1}{sC_{vt}} \cdot I_{DGt} = \sum_t \frac{1}{sC_{vt}} \cdot (H_{Dt}(s) \cdot I_{DGt}) \quad (21)$$

where $H_{Dt}(s)$ is the harmonic detector to detect the t th DG harmonic current ID_{Gt} . It can also be seen that parallel resonant controllers used in the outer loop voltage control in (19) are essentially a set of band-pass filters with narrow bandwidth ω_{ck} and amplified magnitudes K_{ik} . Indeed, the harmonic selective capability has already been embedded in the resonant controllers.

TABLE II: DG UNIT PARAMETERS

Control Parameter	Value
Rated voltage	RM5 60 V
Rated frequency	$f = 60$ Hz
Drop coefficients	$D_p = 1/300; D_v = 1/300; K_G = 1/30;$
Proportional gain	$K_p = 0.11$
Resonant gain	$K(f = 20, K(3) = 15, K(5) = 15, K(7) = 15, K(9) = 10$
Cutoff frequency	$\omega_{c1} = 4 \text{ rad/s} (K = f, 3, 5, 7, \text{ and } 9)$
Inner loop controller	$K_{inner} = 20$
DC link voltage	$V_{dc} = 1000$
Sampling and switching frequency	12 kHz
Circuit parameter	Value
LCL filter	$L_1 = 2 \text{ mH}; L_2 = 3.5 \text{ mH}; C_f = 20 \mu\text{F}$
LC filter	$L_3 = 2 \text{ mH}; L_4 = 0 \text{ mH}; C_f = 20 \mu\text{F}$ (DG unit 1 in Figs. 14 and 15)
Command virtual resistance	$R_1 = 3.5 \Omega$ (DG unit in Figs. 10-13) $R_2 = 11 \Omega$ (DG unit 1 and DG unit 2 in Figs. 14 and 15)

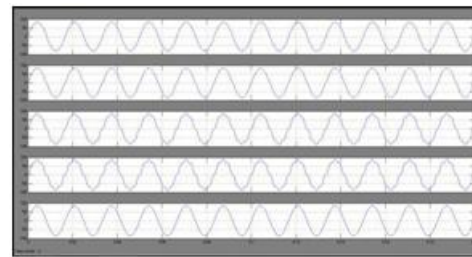


Fig. 10. Harmonic voltage amplification during a single DG unit gridconnected operation (without damping) [from upper to lower: (a) PCC voltage (THD = 4.0%); (b) node 1 voltage (THD = 4.56%); (c) node 3 voltage (THD = 10.91%); (d) node 5 voltage (THD = 12.59%); (e) DG unit filter capacitor voltage (THD = 0.38%)].

Properly, resonant controllers can be further utilized to realize the control of virtual nonlinear capacitor. First, the instantaneous DG voltage reference V_{reff} derived from (6) and (7) is always ripple-free and the fundamental resonant controller can be adopted for V_{reff} tracking. In addition, the regulation of virtual resistor and virtual capacitor mainly focuses on the performance at selected harmonic frequencies. Therefore, parallel harmonic resonant controllers can be utilized to control these virtual impedances. Once the conventional PR controller is separated into two parts, the modified outer loop control scheme is illustrated as follows:

$$I_{inner} = \left(K_{p1} + \frac{2k_{if}\omega_c f^2}{S^2 + 2\omega_c f^S + (\omega f)^2} \right) \cdot (V_{ref} - V_c) + \sum_{k \neq f} \frac{2k_{ik}\omega_c k^2}{S^2 + 2\omega_c k^S + (k\omega f)^2} \cdot (-V_{AD} - V_{Comp} - V_c) \quad (22)$$

Combining (20), (21), and (22) yields

$$I_{inner} = \left(K_{p1} + \frac{2k_{if}\omega_c f^S}{S^2 + 2\omega_c f^S + (\omega f)^2} \right) \cdot (V_{ref} - V_c) - \sum_{t \neq f} \frac{2k_{ik}\omega_c k^S}{S^2 + 2\omega_c k^S + (k\omega f)^2} \cdot (R_V \cdot H_D(s) I_{DG} + V_c) - \left[\sum_{t \neq f} \frac{2k_{ik}\omega_c k^S}{S^2 + 2\omega_c k^S + (k\omega f)^2} \left(\sum_{t \neq f} \frac{(t\omega_f L_2)^2}{S} H_{Dt}(s) \cdot I_{DG} \right) \right] \quad (23)$$

Note that the HD(s) is a harmonic detector, which has 0 db and 0° response at all selected harmonic frequencies and HDt(s) is a selective harmonic detector which only has 0 db and 0° response at the tth harmonic frequency. By further utilizing the harmonic selective feature of harmonic resonant controllers in the PR controller, (23) can be further simplified as

$$I_{inner} = \left(K_{p1} + \frac{2k_{if}\omega_c f^S}{S^2 + 2\omega_c f^S + (\omega f)^2} \right) \cdot (V_{ref} - V_c) - \sum_{t \neq f} \frac{2k_{ik}\omega_c k^S}{S^2 + 2\omega_c k^S + (k\omega f)^2} \cdot (R_V \cdot I_{DG} + V_c) - \left[\sum_{t \neq f} \frac{2k_{ik}\omega_c k^S (k\omega_f L_2)^2}{S^2 + 2\omega_c k^S + (k\omega f)^2} I_{DG} \right] \quad (24)$$

With this modified outer loop controller, the DG unit fundamental voltage tracking and harmonic virtual impedance regulation can be realized separately. The detailed DG controller with the control of virtual nonlinear capacitor is shown in Fig. 9. In the revised controller, the harmonic voltage references associated with virtual resistor and virtual capacitor are only regulated by the harmonic resonant controllers.

It can be seen that the derivative operator in Fig. 8 is avoided in Fig. 9. It is true that the small proportional gain KP1 in (24) still induces some interference between fundamental and harmonic components regulation. However, the proportional gain in the PR controller is normally very small compared to resonant gains. In this paper, a small proportional gain (KP1 = 0.11) is

TABLE III: HARMONIC SPECTRUM OF A GRID- CONNECTED MICROGRID WITHOUT ACTIVE DAMPING (CORRESPONDING TO FIG. 10)

	3rd harmonic	5th harmonic	7th harmonic	9th harmonic	11th harmonic	13th harmonic	THD
PCC voltage	2.00%	2.00%	2.00%	2.00%	0%	0%	4.00%
Node 1 voltage	1.91%	2.41%	2.89%	1.71%	0.05%	0.05%	4.56%
Node 3 voltage	1.65%	2.92%	10.37%	0.74%	0.07%	0.04%	10.91%
Node 5 voltage	1.24%	2.57%	12.31%	2.07%	0.01%	0.02%	12.99%
DG voltage	0.02%	0.04%	0.09%	0.14%	0.15%	0.2%	0.36%

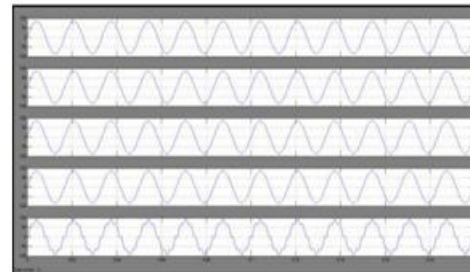


Fig. 11. Harmonic voltage amplification during a single DG unit gridconnected operation (with virtual nonlinear capacitor and resistor based active damping) [from upper to lower: (a) PCC voltage (THD = 4.0%); (b) node 1 voltage (THD = 4.1%); (c) node 3 voltage (THD = 3.7%); (d) node 5 voltage (THD = 3.2%); and (e) DG unit filter capacitor voltage (THD = 5.4%)].

Between the fundamental and the harmonic DG voltage tracking. With aforementioned efforts, the derivative operation is successfully avoided by using the proposed virtual nonlinear capacitor.

V. FUZZY LOGIC CONTROLLER

In FLC, basic control action is determined by a set of linguistic rules. These rules are determined by the system. Since the numerical variables are converted into linguistic variables, mathematical modeling of the system is not required in FC.

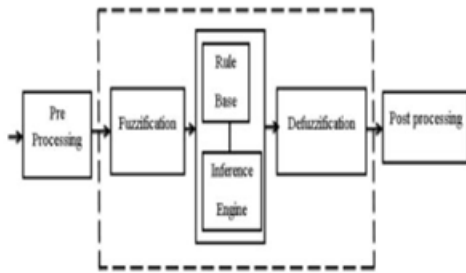


Fig.12.Fuzzy logic controller

The FLC comprises of three parts: fuzzification, interference engine and defuzzification. The FC is characterized as i. seven fuzzy sets for each input and output. ii. Triangular membership functions for simplicity. iii. Fuzzification using continuous universe of discourse. iv. Implication using Mamdani's, 'min' operator. v. Defuzzification using the height method.

TABLE IV: Fuzzy Rules

Change in error	Error						
	NB	NM	NS	Z	PS	PM	PB
NB	PB	PB	PB	PM	PM	PS	Z
NM	PB	PB	PM	PM	PS	Z	Z
NS	PB	PM	PS	PS	Z	NM	NB
Z	PB	PM	PS	Z	NS	NM	NB
PS	PM	PS	Z	NS	NM	NB	NB
PM	PS	Z	NS	NM	NM	NB	NB
PB	Z	NS	NM	NM	NB	NB	NB

Fuzzification:

Membership function values are assigned to the linguistic variables, using seven fuzzy subsets: NB (Negative Big), NM (Negative Medium), NS (Negative Small), ZE (Zero), PS (Positive Small), PM (Positive Medium), and PB (Positive Big). The Partition of fuzzy subsets and the shape of membership $CE(k)$ $E(k)$ function adapt the shape up change in error are normalized by an input scaling factor. In this system the input scaling factor has been designed such that input values are between -1 and +1. The triangular shape of the membership function of this arrangement presumes that for any particular

$E(k)$ input there is only one dominant fuzzy subset. The input error for the FLC is given as

$$E(k) = \frac{P_{ph}(k) - P_{ph}(k-1)}{V_{ph}(k) - V_{ph}(k-1)} \quad (25)$$

$$CE(k) = E(k) - E(k-1) \quad (26)$$

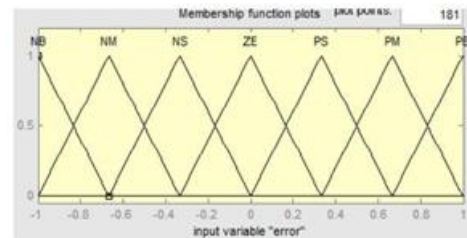


Fig.13.Membership functions

Inference Method:

Several composition methods such as Max-Min and Max-Dot have been proposed in the literature. In this paper Min method is used. The output membership function of each rule is given by the minimum operator and maximum operator. Table 1 shows rule base of the FLC.

Defuzzification:

As a plant usually requires a non-fuzzy value of control, a defuzzification stage is needed. To compute the output of the FLC, „height“ method is used and the FLC output modifies the control output. Further, the output of FLC controls the switch in the inverter. In UPQC, the active power, reactive power, terminal voltage of the line and capacitor voltage are required to be maintained. In order to control these parameters, they are sensed and compared with the reference values. To achieve this, the membership functions of FC are: error, change in error and output

The set of FC rules are derived from

$$u = -[\alpha E + (1-\alpha)*C] \quad (27)$$

Where α is self-adjustable factor which can regulate the whole operation. E is the error of the system, C is the change in error and u is the control variable. A large value of error E indicates that given system is not in the balanced state.

If the system is unbalanced, the controller should enlarge its control variables to balance the system as early as possible. On the other hand, small value of the error E indicates that the system is near to balanced state.

V. VERIFICATION RESULTS

Simulated results have been obtained from a single-phase low voltage microgrid. To emulate the behavior of six kilometers feeder with distributed parameters, a DG unit with an LCL filter is connected to PCC through a ladder network with six identical LC filter units (see Fig. 1). Each LC filter represents 1 km feeder. The parameters of these LC filters are selected to be the same as these in Table I. To provide some passive damping effects to the feeder, the LC filter inductor stray resistance is set to 0.12Ω . The detailed DG unit control parameters are listed in Table II.

A. Single DG Unit Grid-Tied Operation

At first, the performance of a grid-connected DG unit with an LCL filter is examined. The PCC voltage in this simulation is stiff and it has 2.0% distortion at each lower order harmonic frequency (3rd, 5th, 7th, and 9th harmonics).

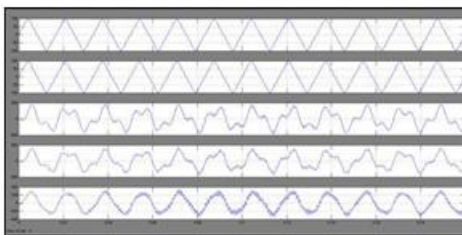


Fig. 14. Harmonic voltage amplification during a single DG unit islanding operation (without damping) [from upper to lower: (a) PCC voltage (THD = 15.2%); (b) node 1 voltage (THD = 14.7%); (c) node 3 voltage (THD = 11.9%); (d) node 5 voltage (THD = 10.5%); and (e) DG unit filter capacitor voltage (THD = 1.6%)].

TABLE V
HARMONIC SPECTRUM OF AN ISLANDING MICROGRID WITHOUT ACTIVE DAMPING (CORRESPONDING TO FIG. 12)

	3rd harmonic	5th harmonic	7th harmonic	9th harmonic	11th harmonic	13th harmonic	THD
PCC voltage	13.19%	2.95%	0.29%	1.66%	6.58%	0.54%	15.19%
Node 1 voltage	11.96%	3.68%	0.39%	1.07%	6.62%	1.06%	14.67%
Node 3 voltage	10.05%	4.35%	1.45%	0.66%	1.09%	0.61%	11.93%
Node 5 voltage	7.54%	3.83%	1.73%	1.76%	5.98%	0.86%	10.51%
DG voltage	0.10%	0.05%	0.02%	0.45%	1.43%	0.2%	1.60%

B. Single DG Unit Islanding Operation

In addition to grid-connected operation, the performance of a single DG unit in islanding operation is also investigated. In this case, the PCC load is a single-phase diode rectifier and it is supplied by the DG unit through long feeder. When the conventional VCM without damping is adopted, the performance of the system is obtained in Fig. 12. Similar to the grid-tied operation, the voltage waveforms at PCC, nodes 1, 3, and 5, and DG unit filter capacitor are shown from channels (a) to (e), respectively.

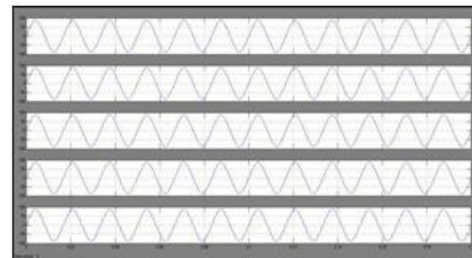


Fig. 15. Harmonic voltage amplification during a single DG unit islanding operation (with virtual nonlinear capacitor and resistor based active damping) [from upper to lower: (a) PCC voltage (THD = 6.1%); (b) node 1 voltage (THD = 6.0%); (c) node 3 voltage (THD = 5.2%); (d) node 5 voltage (THD = 5.3%); and (e) DG unit filter capacitor voltage (THD = 7.1%)].

C. Multiple DG Units Grid-Tied Operation

To verify the circulating harmonic current between multiple DG units, two grid-connected DG units at the same power rating are placed at the receiving end of the feeder.

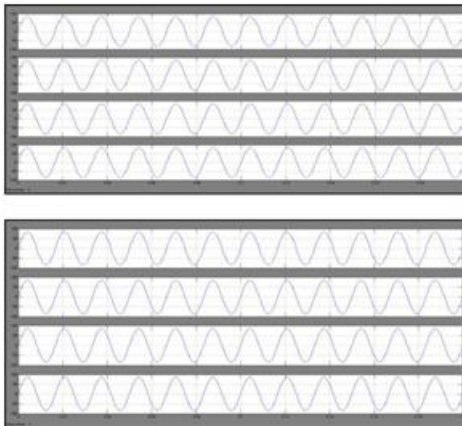


Fig. 16. Harmonic voltage amplification along the feeders (grid-tied operation of two parallel DG units).

VI. CONCLUSION:

In this paper, the impacts of voltage-controlled and current-controlled distributed generation (DG) units to microgrid resonance propagation are compared. To actively mitigate the resonance using DG units, an enhanced DG unit component of the proposed nonlinear virtual impedance is employed to compensate the impact of dg unit LCL filter grid-side inductor. The resistive element is responsible for active damping. With properly controlled dg equivalent harmonic impedance at chosen harmonic frequencies, the proposed method can even eliminate the harmonic circulating current among multiple dg units with mismatched output filter parameters. Here we are using the fuzzy controller compared to other controllers due to its accurate performance. Comprehensive simulations are conducted to substantiate the validity of the proposed method.

REFERENCES:

- [1] H. Akagi, "Active harmonic filters," *Proc. IEEE*, vol. 93, no. 12, pp. 2128–2141, Dec. 2005.
- [2] H. Akagi, H. Fujita, and K. Wada, "A shunt active filter based on voltage detection for harmonic termination for radial power distribution system," *IEEE Trans. Ind. Appl.*, vol. 35, no. 4, pp. 682–690, Jul./Aug. 1995.
- [3] K. Wada, H. Fujita, and H. Akagi, "Consideration of a shunt active filter based on voltage detection for installation on a long distribution feeder," *IEEE Trans. Ind. Appl.*, vol. 38, no. 4, pp. 1123–1130, Jul./Aug. 2002.
- [4] P.-T. Cheng and T.-L. Lee, "Distributed active filter systems (DAFSs): A new approach to power system harmonics," *IEEE Trans. Ind. Appl.*, vol. 42, no. 5, pp. 1301–1309, Sep./Oct. 2006.
- [5] T.-L. Lee and P.-T. Cheng, "Design of a new cooperative harmonic filtering strategy for distributed generation interface converters in an islanding network," *IEEE Trans. Power Electron.*, vol. 42, no. 5, pp. 1301–1309, Sep. 2007.
- [6] T.-L. Lee, J.-C. Li, and P.-T. Cheng, "Discrete frequency-tuning active filter for power system harmonics," *IEEE Trans. Power Electron.*, vol. 24, no. 5, pp. 1209–1217, Apr. 2009.
- [7] T.-L. Lee and S.-H. Hu, "Discrete frequency-tuning active filter to suppress harmonic resonances of closed-loop distribution power system," *IEEE Trans. Power Electron.*, vol. 26, no. 1, pp. 137–148, Dec. 2010.
- [8] N. Pogaku and T. C. Green, "Harmonic mitigation throughout a distribution system: A distributed-generator-based solution," *IEE Proc. Gener. Transmiss. Distrib.*, vol. 153, no. 3, pp. 350–358, May 2006.
- [9] C. J. Gajanayake, D. M. Vilathgamuwa, P. C. Loh, R. Teodorescu, and F. Blaabjerg, "Z-source-inverter-based flexible distributed generation system solution for grid power quality improvement," *IEEE Trans. Energy Convers.*, vol. 24, pp. 695–704, Sep. 2009.
- [10] Y. W. Li, D. M. Vilathgamuwa, and P. C. Loh, "Design, analysis and realtime testing of a controller for multibusmicrogrid system," *IEEE Trans. Power Electron.*, vol. 19, no. 5, pp. 1195–1204, Sep. 2004.